streptavidin-biotin procedure was performed using the histofine SAB (M) kit (Nichirei Co., Tokyo, Japan). After washing in PBS, the sections were exposed for 5 min to tetrahydrochloride (Wako Pure Chemical Industries, Ltd., Osaka, Japan) in 0.05 M Tris buffer, pH 7.6, containing 0.003% hydrogen peroxide. To facilitate visualization of cytoplasmic immunostaining, the slides were counterstained with Mayer hematoxylin. Experiments and control experiments were each performed twice on different days. One author (Y.K.) who had no knowledge of the pathologic diagnosis or any clinical or radiological data determined the MIB-1 labeling index (LI) by counting 1000 tumor cell nuclei. We selected the median value of the MIB-1 LI as the cut-off point, and classified the patients into 2 groups: < 15.8% group, and > 15.8% group. Expression of p53 and EGFR was classified as negative (< 30%) or positive (> 30%) by one of the authors (F.Y.) as we previously reported [8].

Evaluation of survivin expression

The specimens were scored for nuclear and cytoplasmic staining, by 2 authors (H.S. and M.T.) who had no knowledge of the pathological diagnosis or any clinical or radiological data. They counted at least 1000 tumor cells per sample from randomly selected fields at ×400 magnification. Samples in which > 5% of the tumor cells stained positive for survivin (in the nucleus and/or cytoplasm) were recorded as positive for survivin, and samples in which ≤ 5% of the tumor cells stained positive for survivin were scored as negative for survivin, in accordance with previously reported methods [16–18]. The positive specimens were also categorized into 3 groups according to localization of survivin expression: nuclear-positive group (only nucleus positive), cytoplasmic-positive group (only cytoplasm positive), and nuclear-cytoplasmic group (both nucleus and cytoplasm positive).

Statistical analysis

Statistical analyses were performed using the SPSS 11.5 software package for Windows (SPSS INC., Chicago, IL). Correlation between clinicopathological characteristics and localization of survivin expression was calculated using the chi-square test. Cumulative survival curves were estimated using the Kaplan-Meier method. Correlations between survival and survivin localization were calculated using the log-rank test. Multivariate survival analysis was performed using the Cox proportional hazards regression model, which included the following clinicopathological factors: age, sex, extent of resection, MIB-1 labeling index, expression of mutant p53 and EGFR, and survivin localization. In all analyses, a probability value of $P < 0.05$ was considered to indicate statistical significance.

Results

Localization of survivin expression and clinical characteristics of high-grade astrocytomas

All specimens were positive for survivin: nuclear-positive group, 10 cases (20%); cytoplasmic-positive group, 23 cases (45%); nuclear-cytoplasmic group, 18 cases (35%). Figure 1 shows a representative specimen for each group. Table 1 shows the distribution of survivin localization and clinical characteristics for all 51 patients. There was no significant correlation between localization of survivin and any of the clinical factors (age, sex, WHO grade, and extent of resection).

Localization of survivin expression and immunohistochemical factors of high-grade astrocytomas

Of the 51 high-grade astrocytomas examined, positive immunoreactivity for EGFR was observed in 25 cases (49.0%; Table 2), and positive immunoreactivity for p53 was observed in 33 cases (64.7%). The localization of survivin expression did not correlate with the Mib-1 labeling index (P = 0.6798), p53 expression (P = 0.8039), or EGFR expression (P = 0.7431; Table 2).

Both nuclear and cytoplasmic survivin expression correlates with poor prognosis

Univariate analysis using the log-rank test showed no significant difference in survival between the nuclear-positive group and the cytoplasmic-positive group (P = 0.796). However, the nuclear-cytoplasmic group had significantly shorter overall survival than the nuclear-positive group and the cytoplasmic-positive group (P = 0.0001; Figure 2).

Multivariate analysis indicated that survivin localization (nuclear-cytoplasmic group vs. nuclear-positive group or cytoplasmic-positive group) significantly correlated with overall survival (P < 0.001; Table 3). Thus, the data indicates that simultaneous expression of survivin in both the nucleus and cytoplasm is a more reliable predictor of poor prognosis than the other clinicopathological factors in our analysis, including MIB-1 LI, p53 expression and EGFR expression.

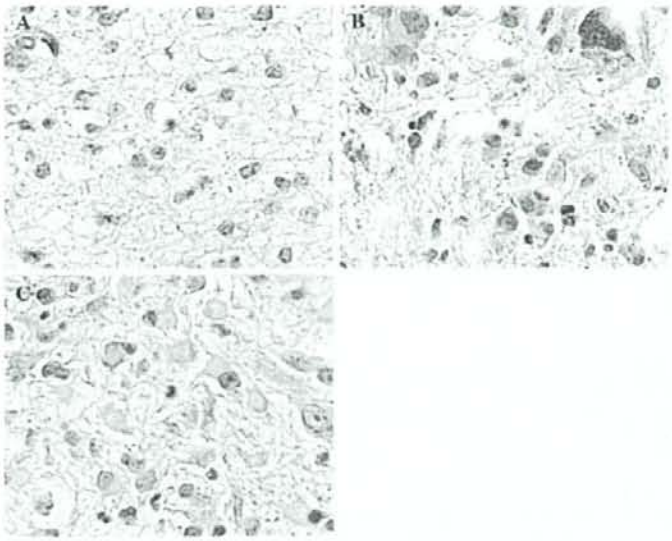

Fig. 1 Immunohistochemical staining for survivin expression in high-grade astrocytomas. A; Expression only in nucleus (nuclear-positive group). B; Expression only in cytoplasm (cytoplasmic-positive group). C; Expression in both nucleus and cytoplasm (nuclear-cytoplasmic group). Original magnification, ×400

Discussion

The present data indicates that simultaneous expression of survivin in both the nucleus and cytoplasm predicts poor prognosis of patients with high-grade astrocytoma. This is the first reported study to evaluate correlation between subcellular localization of survivin and prognosis of high-grade astrocytomas. We and others have previously demonstrated that expression of survivin mRNA or protein is significantly associated with poor prognosis of astrocytic tumors [7–9]. However, in those studies, there was no analysis of the relationship between subcellular localization of survivin and response to treatment. Recent evidence suggests that subcellular localization of survivin also correlates with prognosis of several other malignant tumors. In some malignant tumors, nuclear expression of survivin correlates with unfavorable prognosis, while the nuclear expression in other tumors correlates with favorable prognosis [17–23] Thus, there remains controversy regarding associations between subcellular

Table 1 Localization of survivin expression and clinical characteristics

	Localization of survivin expression				P value
	Nuclear	Cytoplasmic	Nuclear-Cytoplasmic	Total	
Nunber of patients	10	23	18	51	
Age (Median)					
< 56 years	6	12	5	23	0.1701
> 56 years	4	11	13	28	
Sex					
Male	4	13	12	29	0.3934
Female	6	10	6	22	
WHO grade					
III	5	9	5	19	0.4914
IV	5	14	13	32	
Resection					
Total	2	3	1	6	0.6841
Subtotal	0	2	2	4	
Partial	8	18	15	41	

Statistical analysis performed using chi-square test

Table 2 Localization of survivin expression and immunohistochemical factors

	Localization of survivin expression				P value
	Nuclear	Cytoplasmic	Nuclear-Cytoplasmic	Total	
MIB-1 labeling index					
< 15.8 %	6	10	9	25	0.6798
> 15.8 %	4	13	9	26	
p53					
negative (<30 %)	4	7	7	18	0.8039
positive (>30 %)	6	16	11	33	
EGFR					
negative (<30 %)	5	13	8	26	0.7431
positive (>30 %)	5	10	10	25	

Statistical analysis performed using chi-square test

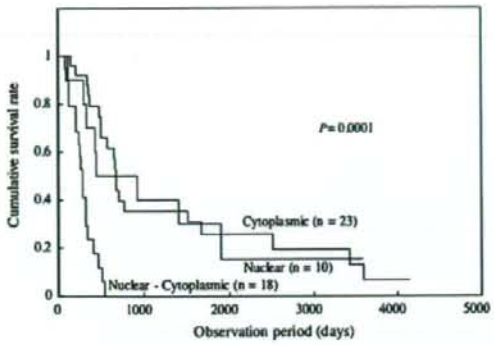

Fig. 2 Kaplan-Meier curves for the overall survival rates of high-grade astrocytoma patients with survivin expression only in the cytoplasm of tumor cells (cytoplasmic-positive group), only in the nucleus (nuclear-positive group), or in both the nucleus and cytoplasm (nuclear-cytoplasmic group). There was no significant difference in survival between the nuclear-positive group and the cytoplasmic-positive group (P = 0.796). However, the nuclear—cytoplasmic group had significantly shorter overall survival than the nuclear-positive group and the cytoplasmic-positive group (P = 0.0001)

localization of survivin and prognosis of malignant tumors.

The present results indicate that survivin expression limited to only the nucleus or cytoplasm does not correlate with prognosis of high-grade astrocytoma, and also indicate that simultaneous expression of survivin in both the nucleus and cytoplasm significantly correlates with poor prognosis of high-grade astrocytoma. There are no previous reports of analysis of the effect of simultaneous oncogenic protein expression in both the nucleus and cytoplasm on response to treatment

Table 3 Multivariate Analysis of Prognostic Factors

Factor	Survival		
	Hazard ratio	P value	95% CI
Age	2.277	0.034*	1.064–4.872
Sex (Female vs. Male)	1.516	0.248	0.748–3.071
Resection (Partial vs. Total + Subtotal)	2.841	0.061	0.955–8.456
MIB-1 index (>15.8% vs. ≤ 15.8 %)	1.806	0.110	0.874–3.731
p53 (>30% vs. <30%)	0.689	0.295	0.343–1.384
EGFR (>30% vs. <30%)	0.741	0.428	0.353–1.556
Survivin localization†	3.933	<0.001*	1.847–8.373

†Both nucleus and cytoplam positive vs. only nucleus or cytoplasm positive

Statistical analysis performed using Cox proportional hazards regression model; *$P < 0.05$

in malignant tumor patients. However, some reports suggest that differently localized oncogenic proteins interact and work cooperatively in tumorigenesis [24]. Therefore, the present approach is novel, and the present report represents a significant contribution to studies of the effect of subcellularly localized oncogenic protein on tumorigenesis in malignant tumors.

There have been several studies of correlation between the subcellular localization of survivin, its splice variants and their bifunctional roles; i.e., anti-apoptosis and promotion of mitosis [11–15]. The isoforms survivin and survivin-2B are found predominantly in the cytoplasm, whereas the survivin-deltaEX3 isoform is preferentially localized in the nucleus [11]. These differences in subcellular localization between the splice variants of survivin are associated with their functions in cell survival and cell division [11–15, 25]. One possibility is that the nuclear pool of survivin is involved in regulation of cell division and promotion of cell proliferation, whereas the cytoplasmic pool of survivin participates in control of cell survival (anti-apoptotic function) but not cell division [26].

Recently, Xie et al. [27] studied the pattern of subcellular survivin expression in 30 primary and 26 secondary glioblastomas. In their report, they hypothesized that the high frequency of cytoplasmic survivin in glioblastoma may strengthen the barriers to cell apoptosis, thus accelerating the oncogenic process. On the other hand, they found that the majority of glioblastomas had aneuploid DNA content, and found a close association between nuclear survivin positivity and tumor aneuploidy. These findings suggest that nuclear-localized survivin in glioblastomas influences mitotic events and subsequently promotes chromosomal instability. They also indicate that these different forms of survivin (nuclear and cytoplasmic) have different effects on the malignant behavior of human glioma cells, and that they can have a profound effect on the development and/or progression of primary and secondary glioblastomas. Such findings suggest that simultaneous expression of survivin in both the nucleus and cytoplasm of cells in high-grade astrocytoma results in cooperative aggressive anti-apoptotic activity and chromosomal instability, plays an important role in acquisition of more malignant characteristics, and is involved in resistance to post-operative adjuvant therapy.

However, the present study has a limitation. The study population was rather small at 51 patients; larger prospective studies are needed.

In conclusion, the present study is the first reported evaluation of the prognostic significance of

simultaneous survivin expression in both nucleus and cytoplasm in high-grade astrocytomas. We found that simultaneous expression of survivin was an important prognostic factor for patients who underwent surgery and adjuvant radiation therapy. We conclude that the subcellular localization of survivin expression (especially simultaneous localization in both the nucleus and cytoplasm) is a reliable prognostic factor of high-grade astrocytomas.

Acknowledgement This study was supported in part by a Grant-in-Aid for Scientific Research from the Ministry of Education, Culture, Sports, Science and Technology of Japan.

References

1. Berg G, Blomquist E, Cavallin-Stahl E (2003) A systematic overview of radiation therapy effects in brain tumours. Acta Oncol 42:582–588
2. Nieder C, Andratschke N, Wiedenmann N et al (2004) Radiotherapy for high-grade gliomas. Does altered fractionation improve the outcome?. Strahlenther Onkol 180:401–407
3. Stewart LA (2002) Chemotherapy in adult high-grade glioma: a systematic review and meta-analysis of individual patient data from 12 randomized trials. Lancet 359:1011–1018
4. Tanaka K, Iwamoto S, Gon G et al (2000) Expression of survivin and its relationship to loss of apoptosis in breast carcinomas. Clin Cancer Res 6:127–134
5. Schlette EJ, Medeiros LJ, Goy A et al (2004) Survivin expression predicts poorer prognosis in anaplastic large-cell lymphoma. J Clin Oncol 22:1682–1688
6. Salz W, Eisenberg D, Plescia J et al (2005) A survivin gene signature predicts aggressive tumor behavior. Cancer Res 65:3531–3534
7. Chakravarti A, Noll E, Black PM et al (2002) Quantitatively determined survivin expression levels are of prognostic value in human gliomas. J Clin Oncol 20:1063–1068
8. Kajiwara Y, Yamasaki F, Hama S et al (2003) Expression of survivin in astrocytic tumors: correlation with malignant grade and prognosis. Cancer 97:1077–1083
9. Uematsu M, Ohsawa I, Aokage T et al (2005) Prognostic significance of the immunohistochemical index of survivin in glioma: a comparative study with the MIB-1 index. J Neurooncol 72:231–238
10. Konstantinidou AE, Korkolopoulou P, Patsouris E (2005) Apoptotic markers for primary brain tumor prognosis. J Neurooncol 72:151–156
11. Mahotka C, Liebmann J, Wenzel M et al (2002) Differential subcellular localization of functionally divergent survivin splice variants. Cell Death Differ 9:1334–1342
12. Rodriguez JA, Span SW, Ferreira CG et al (2002) CRM1-mediated nuclear export determines the cytoplasmic localization of the antiapoptotic protein Survivin. Exp Cell Res 275:44–53
13. Caldas H, Jiang Y, Holloway MP et al (2005) Survivin splice variants regulate the balance between proliferation and cell death. Oncogene 24:1994–2007
14. Caldas H, Honsey LE, Altura RA (2005) Survivin 2alpha: a novel Survivin splice variant expressed in human malignancies. Mol Cancer 4:11
15. Song Z, Wu M (2005) Identification of a novel nucleolar localization signal and a degradation signal in Survivin-deltaEx3: a potential link between nucleolus and protein degradation. Oncogene 24:2723–2734
16. Kawasaki H, Altieri DC, Lu CD et al (1998) Inhibition of apoptosis by survivin predicts shorter survival rates in colorectal cancer. Cancer Res 58:5071–5074
17. Grabowski P, Kuhnel T, Muhr-Wilkenshoff F et al (2003) Prognostic value of nuclear survivin expression in oesophageal squamous cell carcinoma. Cancer 88:115–119
18. Vischioni B, van der Valk P, Span SW et al (2004) Nuclear localization of survivin is a positive prognostic factor for survival in advanced non-small-cell lung cancer. Ann Oncol 15:1654–1660
19. Fields AC, Cotsonis G, Sexton D et al (2004) Survivin expression in hepatocellular carcinoma: correlation with proliferation, prognostic parameters, and outcome. Mod Pathol 17:1378–1385
20. Martinez A, Bellosillo B, Bosch F et al (2004) Nuclear survivin expression in mantle cell lymphoma is associated with cell proliferation and survival. Am J Pathol 164:501–510
21. Okada E, Murai Y, Matsui K et al (2001) Survivin expression in tumor cell nuclei is predictive of a favorable prognosis in gastric cancer patients. Cancer Lett 163:109–116
22. Kennedy SM, O'Driscoll L, Purcell R et al (2003) Prognostic importance of survivin in breast cancer. Br J Cancer 88:1077–1083
23. Trieb K, Lehner R, Stulnig T et al (2003) Survivin expression in human osteosarcoma is a marker for survival. Eur J Surg Oncol 29:379–82
24. Macaluso M, Montanari M, Noto PB et al (2006) Nuclear and cytoplasmic interaction of pRb2/p130 and ER-[beta] in MCF-7 breast cancer cells. Ann Oncol 17(Supplement 7:vii27–vii29
25. Li F (2005) Role of survivin and its splice variants in tumorigenesis. Br J Cancer 92:212–216
26. Li F, Yang J, Ramnath N et al (2005) Nuclear or cytoplasmic expression of survivin: what is the significance? Int J Cancer 114:509–512
27. Xie D, Zeng YX, Wang HJ et al (2006) Expression of cytoplasmic and nuclear Survivin in primary and secondary human glioblastoma. Br J Cancer 94:108–114

Geminin: A Good Prognostic Factor in High-grade Astrocytic Brain Tumors

Prabin Shrestha, MD
Taiichi Saito, MD
Seiji Hama, MD, PhD
Muhamad T. Arifin, MD
Yoshinori Kajiwara, MD, PhD
Fumiyuki Yamasaki, MD, PhD
Toshikazu Hidaka, MD
Kazuhiko Sugiyama, MD, PhD
Kaoru Kurisu, MD, PhD*

Department of Neurosurgery, Graduate School of Biomedical Sciences, Hiroshima University, Hiroshima, Japan.

BACKGROUND. Geminin is a nuclear protein that belongs to the DNA replication inhibitor group. It inhibits DNA replication by preventing Cdt1 from loading minichromosome maintenance protein onto chromatin, as is required for DNA replication. For this study, the authors investigated geminin expression in high-grade astrocytic tumors, including anaplastic astrocytoma (AA) and glioblastoma multiforme (GBM), with a view to predicting clinical outcomes on this basis in patients with these malignant brain tumors.

METHODS. Immunohistochemistry was used to detect geminin expression in 51 patients with high-grade astrocytic tumors (19 AA and 32 GBM). Samples were categorized by taking the median value as the cut-off point for constructing Kaplan-Meier curves. The relation of geminin expression to clinical outcome in these malignant brain tumors was analyzed by using the Kaplan-Meier method and a Cox proportional hazards regression model.

RESULTS. Geminin was expressed in all high-grade astrocytomas (mean geminin labeling index [LI], 24.90%). Kaplan-Meier curves showed that the group with higher geminin LI (≥22.50%) had a better prognosis than the group with lower LI (<22.50%; $P = .0296$). Similarly, the Cox regression analysis showed that geminin expression has a significant correlation with survival in patients with high-grade astrocytoma ($P = .0278$), especially in an early stage.

CONCLUSIONS. Although it is an inhibitor of DNA proliferation and, thus, is a cell cycle inhibitor, geminin expression was found in all malignant astrocytic tumors. The geminin LI was a significant predictive factor of outcomes in patients with high-grade astrocytoma, with higher expression indicating a good prognosis. *Cancer* 2007;109:949–56. © *2007 American Cancer Society.*

KEYWORDS: Geminin, MIB-1, high-grade astrocytoma, immunohistochemistry.

Human malignant gliomas grow diffusely and invade surrounding normal brain tissue. Surgical removal of the entire tumor often is difficult, and irradiation often is administered as adjuvant therapy for the treatment of incompletely resected tumors. However, to date, the clinical effectiveness of irradiation has been limited. In almost all patients, these high-grade tumors are refractory to treatment, and the patients die from brain herniation caused by unrestrained tumor growth.[1] The median survival of patients with malignant glioma is <2 years despite extensive and multidisciplinary treatment.

Geminin is a 25-kDa nuclear protein and has a DNA replication-inhibitory function. Its action is mainly through negatively regulating the function of Cdt1, which helps in the formation of prereplication complex (pre-RC) by loading minichromosome maintenance protein (Mcm2-Mcm7) onto chromatin.[2–10] In addition, DNA polymerase binds to this complex and initiates DNA synthesis in S-phase. This process repeats constantly and limits DNA replication

Supported by a grant from A Grant-in-Aid for Scientific Research from the Ministry of Education, Culture, Sports, Science, and Technology of Japan.

Address for reprints: Kaoru Kurisu, MD, PhD, Department of Neurosurgery, Graduate School of Biomedical Sciences, Hiroshima University, 1-2-3, Kasumi, Minami-ku, Hiroshima 734-8551, Japan; Fax: (011) 81-82-257-5229; E-mail: prabinshr@hiroshima-u.ac.jp

Received August 2, 2006; revision received November 6, 2006; accepted November 28, 2006.

DOI 10.1002/cncr.22474
Published online 29 January 2007 in Wiley InterScience (www.interscience.wiley.com).

to once per cycle. To maintain this process, the level of geminin fluctuates at different stages of the cycle; geminin level is at its lowest and is almost absent in G1-phase but is high in S-phase and G2-phase and in the initial stage of M-phase.

Therefore, geminin is responsible not only for the regulation of the cell cycle but also for the genomic integrity of cells thus formed. From these observations, it was believed that geminin likely would have tumor-suppressive functions. However, previous reports have demonstrated that the expression of geminin rises with increasing tumor grade,[11–16] leading to a poor prognosis in a variety of cancer patients, eg, breast cancer and renal cell carcinoma.[17,18] Thus there has been a discrepancy between normal molecular function and the outcomes of clinical studies of geminin in many cancers.

Although the effect of geminin expression on clinical prognosis in a number of malignant tumors has been studied, its effect on astrocytic tumors has not yet been investigated. Moreover, previous studies have not related geminin expression to different treatment modalities, for example, radiotherapy. All of our patients received radiotherapy after surgery as a standard treatment protocol for high-grade astrocytomas.[19,20] For the current study, therefore, we retrospectively examined the expression of geminin in high-grade astrocytic tumors (anaplastic astrocytoma [AA], World Health Organization [WHO] grade III; and glioblastoma multiforme [GBM], WHO grade IV) in relation to clinical prognosis, and we also analyzed at the relation between geminin expression and radiosensitivity.

MATERIALS AND METHODS

Tumor Specimens

The tissue samples were collected during surgery, and all tumor specimens were fixed routinely in 10% buffered formalin and embedded in paraffin, which were obtained from the research laboratory of the Department of Neurosurgery, Hiroshima University, Hiroshima, Japan. Samples were used with the prior informed consent, which was obtained before surgery, of the patients or their guardians.

Clinical Data

To standardize the study and to make it more specific, only patients with high-grade astrocytoma were investigated. Specimens from 51 patients with high-grade astrocytoma were obtained (WHO grades III and IV). In addition, geminin expression in 20 specimens of diffuse astrocytoma (low-grade glioma, WHO grade II) was examined purely for comparison with geminin expression in high-grade gliomas. Pilocytic astrocytomas (WHO grade I) and astrocytomas of the infratentorial region were excluded from the study. We also excluded other types of gliomas, such as oligodendroglioma, ependymoma, ganglioglioma, etc, and gliomas that originated in the thalamus. The included patients underwent surgery between September 1990 and May 2005. Treatment for all patients was primary surgery and radiation therapy. Chemotherapy was not taken into consideration, because as it was not administered uniformly in all patients; and, unlike radiotherapy, it has not yet been proven that chemotherapy prolongs survival in patients with these tumors.[19,20] Details of the 51 patients are shown in Table 1. The mean survival was 29.81 months (range, 3.07–156.63 months).

TABLE 1
Clinical Details of 51 Patients With High-grade Astrocytoma

Parameter	No. of patients
Age, y	
Range	7–72
Mean ± SD	47.98 ± 18.78
Sex	
Men	29
Women	22
Grade	
III	19
IV	32
Tumor resection	
Total	3
Gross total	4
Subtotal	5
Partial	32
Biopsy	7
Follow-up, mo	
Range	3.07–156.63
Mean ± SD	29.30 ± 35.57

SD indicates standard deviation.

Immunohistochemistry

Histologic diagnoses and other information on all tumors were obtained from hospital records. Histologic diagnostic subtypes were defined and categorized according to the WHO criteria and guidelines by 1 of the authors (K.S.). Four-micrometer tissue sections were deparaffinized with xylene, and antigen retrieval was carried out by using the heat-induced epitope retrieval method with citrate buffer solution, pH 6.0. Endogenous peroxidase blocking was carried out by dipping the slides into a solution made by mixing 10 mL of 30% H_2O_2 and 90 mL of 99% methanol for 30 minutes. After each step, the slides were rinsed

and washed with phosphate-buffered saline solution, pH 7.5, 3 times for 5 minutes each. An indirect method of immunostaining, the labeled streptavidin biotin (SAB) method, was employed for antibody incubation, using the histofine SAB kit (Nichirei Company. Tokyo, Japan). The antibody used for geminin was geminin (FL-209), which is a rabbit polyclonal antibody (Santa Cruz Biotechnology, CA) raised against geminin of human origin, at 1:200 dilution. Similarly, the primary antibody for Ki-67 was mouse monoclonal antibody (MIB-1; Immunotech, Marseille, France) at 1:50 dilution. Primary antibody incubation was performed overnight at 4°C, followed by incubation for 30 minutes in secondary antibody (biotinylated secondary antibody, SAB kit; Nichirei Company). Slides were treated with Mayer hematoxylin as a counterstain for better cytoplasmic visualization and then mounted with coverslips for storage purposes.

The slides were evaluated for geminin labeling index (LI) by 2 of the authors, who had no any prior knowledge of the histologic diagnosis or other clinical records: The numbers of positive cells per 1000 were counted in each sample at ×400 magnification under a microscope. A third author estimated the MIB-1 LI by counting the positive nuclei per 1000 tumor cells in each sample in the same manner.

Statistical Analysis

Statistical analyses were performed using the software package SPSS (Statistical Package for the Social Sciences; version 11.5 for Windows). After calculating the geminin LI for all samples by simple counting, as described above, the mean and median values were calculated.

Differences in geminin expression at different stages of tumor progression (grades II, III, and IV) in astrocytic brain tumors were assessed by using 1-way analysis of variance (ANOVA). Post-hoc tests were performed using the Scheffe test.

Survival was measured in months from the date of first surgery to the date of death for patients who died or the date of last follow-up for patients who remained alive. The Kaplan-Meier (KM) method was used to assess survival against geminin expression. The median geminin LI was taken as the cut-off point for dividing the samples into 2 categories (less than and greater than the median). Survival and life/death status were plotted against the geminin LI; then, the KM curves were prepared. The log-rank test was used in a univariate analysis to evaluate statistical significance.

A multivariate analysis with 95% confidence intervals (95% CIs) was performed comparing several prognostic variables for survival using the Cox proportional hazards regression model. The prognostic continuous variables were age, geminin LI, MIB-1 LI; and the prognostic categorical variables were sex, tumor grade, and extent of tumor resection. All P values $<.05$ were considered statistically significant. A correlation analysis between the 2 factors age and geminin expression was carried out as a bivariate correlation analysis using the Pearson test.

TABLE 2
Immunohistochemical Findings in 51 Patients With High-grade Astrocytoma

Parameter	Value	%
Geminin		
No. positive	51	100
Mean %	24.90	
Median %	22.50	
No. <22.50%	25	49.02
No. >22.50%	26	50.98
MIB-1		
No. positive	51	100
Mean %	18.18%	
Median %	15.58%	
No. <15.53%	25	49.02
No. >15.53%	26	50.98

RESULTS

Geminin Immunohistochemistry

All 51 clinical samples (100%) showed positive staining for geminin. The mean geminin expression (LI) was 24.90% per high-power field (range, 1.94–68.75% per high-power field), and the median geminin LI was 22.50% per high-power field. Details of the immunohistologic findings are provided in Table 2. Among the 20 patients who had low-grade (grade II) astrocytic tumors, 5 patients (25%) did not have a single positive cell, and the remaining 15 patients (75%) had positive staining. The mean geminin expression (LI) for these low-grade tumors was 11.27% (median, 3.01%). Figure 1 displays representative photomicrographs of geminin immunostaining.

Geminin Expression and Age

Correlation analysis between the factors age and the geminin expression was done by using the bivariate Pearson correlation test, which showed no significant correlation ($P = .187$), suggesting that there is no significant correlation between age and geminin expression.

Geminin Expression and Tumor Grade

Changes in geminin expression over the course of tumor progression were analyzed and are shown in

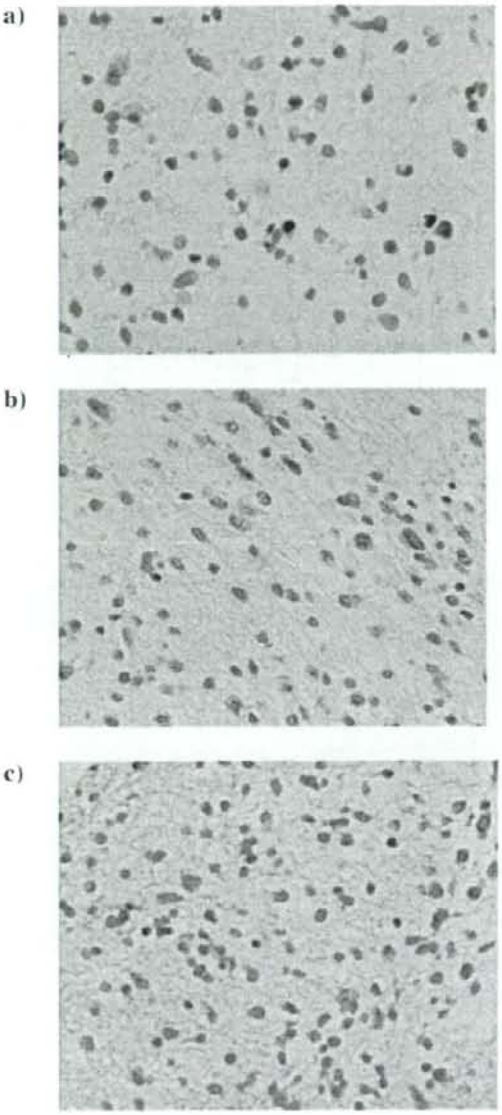

FIGURE 1. Immunohistochemical staining for geminin expression in high-grade astrocytomas. These slides show geminin-negative staining in low-grade astrocytoma (a), geminin-positive staining in low-grade astrocytoma (b), and geminin-positive staining in high-grade astrocytoma (c).

Figure 2. Geminin expression increased significantly as tumors progressed through each step from 1 grade to another grade (from grade II to grade III and from

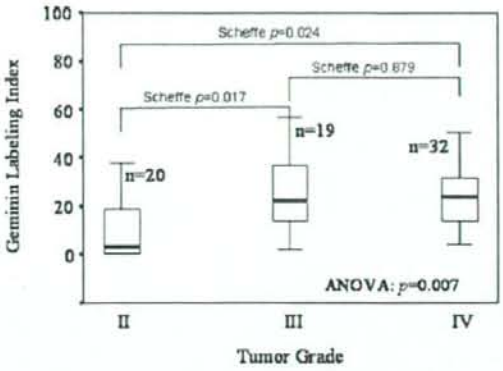

FIGURE 2. Differences in geminin expression over tumor progression in each step from 1 grade to another (grade II, III, and IV). Upper and lower limits of the boxes and the line across the boxes indicate the 75th and 25th percentiles and the median, respectively; upper and lower horizontal lines indicate the 90th and 10th percentiles, respectively. An analysis of variance (ANOVA) between the groups showed statistical significance ($P = .007$). Geminin expression was much higher in grade III and IV tumors compared with grade II tumors (post-hoc Scheffe test; $P = .017$ and $P = .024$, respectively), although there was no statistically significant difference in geminin expression between grade III tumors and grade IV tumors (post-hoc Scheffe test; $P = .879$).

grade III to grade IV; $P = .007$; ANOVA between groups). The Scheffe post-hoc test showed a significant difference in geminin expression between grade II and III tumors and grade II and IV tumors ($P = .017$ and $P = .024$, respectively). However, we observed no significant differences in geminin expression between grade III tumors and grade IV tumors ($P = .879$). Therefore, our current results demonstrated that higher grade tumors have higher geminin expression in astrocytic brain tumors, especially in the early stage of tumor progression.

Tumor Grade and Prognosis

We tried to perform the survival analysis of grade III tumors versus grade IV tumors without noting geminin expression. Our analysis showed, as expected, that the survival of patients with AA was significantly better than the survival of patients with GBM ($P = .0080$) (Fig. 3). Therefore, the correlation between geminin expression and prognosis was studied separately in the AA group and the GBM group.

Geminin Expression and Prognosis

We examined the cumulative survival of 2 groups of patients according to the geminin LI (higher than the

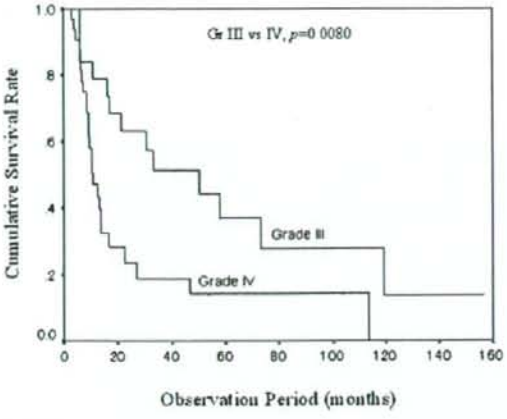

FIGURE 3. This Kaplan-Meier survival curve illustrates the cumulative survival rate of patients by tumor grade (astrocytoma grade [Gr] III vs Gr IV). Survival was significantly better in patients who had anaplastic astrocytoma (Gr III) compared with patients who had glioblastoma multiformes (Gr IV; $P = .0080$).

median value [>22.50%] and lower than the median value [<22.50%]) in the patients with high-grade astrocytic brain tumors (AA and GBM) by using the KM method. The group that had higher geminin expression had a significantly better survival rate compared with the group that had lower geminin expression ($P = .0296$) (Fig. 4a). To test the significance of geminin expression further in the prediction of the clinical outcome of these malignant astrocytomas, Cox multiple regression analysis was used to compare the contribution of the geminin LI with that of the other variables mentioned above. The geminin LI ($P = .0278$) and tumor grade ($P = .0436$) were identified as significant factors for predicting clinical outcomes, as shown in Table 3.

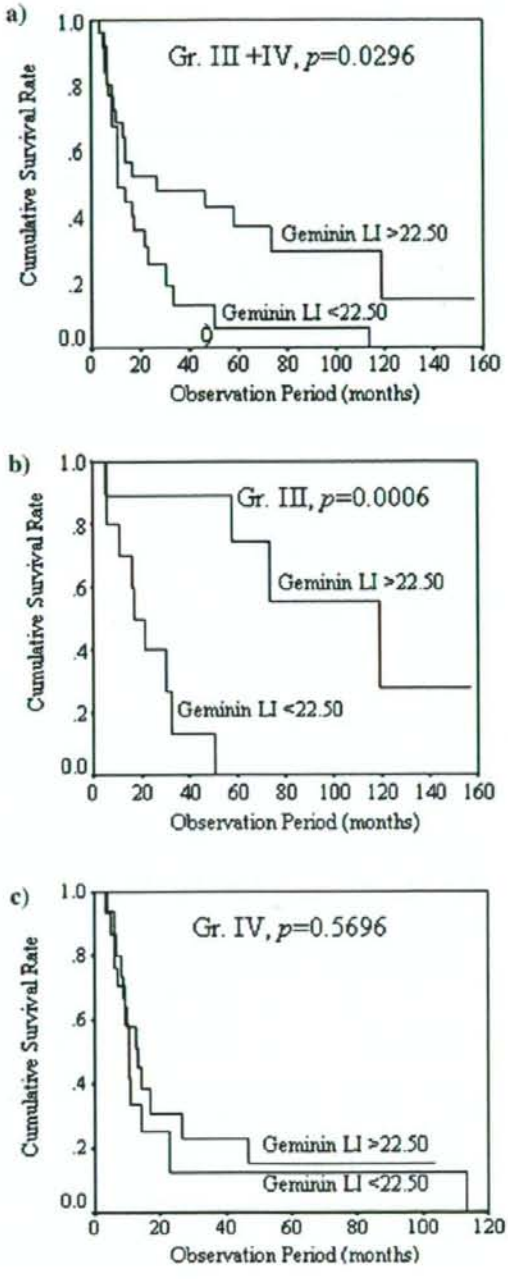

FIGURE 4. Kaplan-Meier survival curves. (a) Cumulative survival rates for patients with high-grade astrocytoma according to the geminin expression labeling index (LI). Survival was significantly better in the group that had higher geminin expression (LI, ≥22.50) compared with the group that had lower geminin expression (LI, <22.50; $P = .0296$). (b) Cumulative survival rates for patients with grade III (Gr III) astrocytoma according to the geminin expression LI. Survival was significantly better in the group that had higher geminin expression (LI, ≥22.50) compared with the group that had lower geminin expression (LI, <22.50; $P = .0006$). (c) Cumulative survival rates for patients with Gr IV astrocytoma according to the geminin expression LI. Survival was better in the group that had higher geminin expression (LI, ≥22.50) compared with the group that had lower geminin expression (LI, <22.50), although the difference was not statistically significant ($P = .5696$).

TABLE 3
Cox Regression Multivariate Analysis for Survival

	Survival		
Factors	HR	P	95% CI
Age	1.0000	.9976	0.9773–1.0232
Sex (men/women)	1.8322	.1027	0.8855–3.7909
Tumor grade (III/IV)	2.2269	.0436	1.0233–4.8462
Tumor resection (T/GT/ST/P/B)	1.1116	.5755	0.7675–1.6098
Geminin LI	0.9658	.0278	0.9363–0.9962
MIB-1 LI	0.9971	.8117	0.9738–1.0210

HR indicates hazard ratio; 95% CI, 95% confidence interval; T, total; GT, gross total; ST, subtotal; P, partial, B, biopsy; LI, labeling index.

To confirm the prognostic significance of geminin expression, we compared patients with AA and patients with GBM separately by using KM curves. The group that had higher geminin expression had a better survival rate than the group that had lower geminin expression in both patients with AA and patients with GBM, whereas a statistical significance was observed only in patients with AA (Fig. 4b) ($P = .0006$) and not in patients with GBM (Fig. 4c) ($P = .5696$). Therefore, we observed that higher geminin expression resulted in better survival rates in patients with high-grade tumors, especially in the early stage of malignant progression of astrocytic brain tumors.

DISCUSSION

Previous studies have found that geminin is expressed highly in a number of malignant conditions, including breast cancer, colorectal cancer, cervical cancer, renal cell carcinoma, oligodendroglioma, and others.[11–16] Geminin is a protein that blocks the rereplication of the gene in the same cycle. It is present in the S-, G2-, and M-phases of the cell cycle but is absent in G1-phase; thus, it is the S/G2/M-phase marker. Its absence indicates a lack of cell cycle progression, and its high expression indicates that cells are progressing rapidly through the S-, G2-, and M-phases and are engaged in DNA synthesis and, thus, cell division. It was mentioned above that, in highly proliferating cells, G1-phase becomes very short, and many cells in this state are in S-, G2-, or M-phase. Thus, more geminin is detected in immunostaining of the tissue of highly proliferating cells, ie, tissues from higher grade tumor. Furthermore, previous studies have shown that the replication licensing factors, like minichromosome maintenance factor and geminin, are up-regulated in the early stages of tumorigenesis and malignant progression.[11,16] Therefore, it has been pointed out that geminin has a causal effect on the carcinogenesis of different tumors, especially in the early stages of carcinogenesis. In patients oligodendroglioma, it also was shown that geminin over-expression had an influence on the progression of tumors from low grade to high grade.[12] These results are consistent with our data, which show that higher grade tumors have higher geminin expression levels, especially during the stage of early progression of malignancy.

Another previous study examined the effect of geminin expression on the overall survival of patients with breast cancer[17]; and those authors demonstrated that the higher expression of geminin was a poor prognostic marker in patients with breast cancer. Yet another study examined the relation of geminin expression to the clinical outcome of patients with renal cell carcinoma and showed the same trend[18]: higher geminin expression was a poor prognostic marker. Surprisingly, the data from our investigation on the relation between geminin expression and survival in patients with high-grade astrocytic tumors contradict those previous findings: Greater frequency of geminin expression is associated with longer survival and, thus, with a better prognosis compared with lower geminin expression (Fig. 4a, Table 3). This trend was similar in both patients with AA and patients with GBM when they were analyzed separately, whereas statistical significance was observed only in patients with AA but not in patients with GBM, suggesting that the geminin LI was a significant predictor of better survival outcomes in patients with high-grade astrocytomas, especially in the early stage of malignant transformation (grade III) (Fig. 4b,c).

A possible reason for these opposing results may lie in differences in the treatments provided. All of our patients both underwent surgery and received radiotherapy as the standard treatment protocol for high-grade astrocytoma. This suggests the possibility that over-expression of geminin may increase radiosensitivity, leading to a better prognosis after radiotherapy, even though geminin expression rises with increasing tumor grade.

In a previous investigation of geminin expression in a series of human normal and cancer cell lines and human primary cancers, it was observed that geminin over-expression stimulated cell cycle progression and proliferation in both normal cells and cancer cells.[13] In that study, in 5 of 6 patients with rectal cancer, the expression of geminin was reduced significantly by chemoradiotherapy, thus suggesting that cells expressing high levels of geminin may be

more sensitive to radiotherapy. However no direct evidence for this heightened sensitivity was presented. We believe that our current study may be the first to suggest an explicit effect of geminin expression on the radiosensitivity of a cancer.

In both normal cells and cancer cells, as discussed above, the geminin level is lowest and almost absent in G1-phase but is high in S-phase and G2-phase and in the initial stage of M-phase. In cancer cells, however, it has been reported that the overexpression of geminin accelerates the cell cycle from the G1-phase to the S-phase, shortening G1-phase and reducing the number of cells in this phase, thus leading to an accumulation of cells in S-phase.[13] The results of clonogenic survival assays clearly indicate that cells synchronized at the M-phase or at the early S-phase are the most radiosensitive, and cells in G1-phase are comparatively radioresistant.[21,22] From these observations, we propose that the higher the expression of geminin, the higher the proportion of cells in phases other than G1 of the cell cycle, resulting in higher radiosensitivity. Therefore, patients who have high-grade astrocytoma patients with overexpressed geminin have favorable outcomes after surgery and radiation therapy.

Some limitations of this study should be acknowledged. First, we used a retrospective design, and a prospective study will be needed to confirm our findings. Second, this was a small study that included only 51 patients with high-grade glioma. Given the postulated effect of a treatment modality, the relation between geminin expression and outcomes when other treatment modalities for brain tumor are involved needs to be explored. Furthermore, we examined only the expression of geminin and MIB-1, and the expression of other molecules, such as p16, p53, epidermal growth factor receptor, etc, may modify the effect of geminin expression on these high-grade tumors. In addition, we have not determined whether the geminin in high-grade astrocytoma is a mutant type or a wild type, and the effect of geminin on the cell cycle of these malignancies may be altered depending on this determination. Finally, it would not be fair to conclude that geminin expression improves radiosensitivity without using a comparison group. We recommend radiotherapy for all of our patients with high-grade glioma after they have undergone surgery, according to the standard protocol for brain tumor management. Therefore, we did not have a control group of patients who did not receive radiotherapy for a comparison study.

In conclusion, the current results indicated that, like what has been observed in other malignancies, geminin is expressed highly in high-grade astrocytic tumors compared with low-grade astrocytic tumors. However, higher expression of geminin in high-grade astrocytomas indicates a more favorable outcome and longer survival in patients who have received radiotherapy after surgery as a standard treatment protocol.

REFERENCES

1. Giangaspero F, Burger PC. Correlations between cytologic composition and biologic behavior in the glioblastoma multiforme. A postmortem study of 50 cases. *Cancer.* 1983; 52:2320–2333.
2. Nishitani H, Lygerou Z. Control of DNA replication licensing in a cell cycle. *Genes Cells.* 2002;7:523–534.
3. Nishitani H, Taraviras S, Lygerou Z, Nishimoto T. The human licensing factor for DNA replication Cdt1 accumulates in G1 and is destabilized after initiation of S-phase. *J Biol Chem.* 2001;276:44905–44911.
4. Eward KL, Obermann EC, Shreeram S, et al. DNA replication licensing in somatic and germ cells. *J Cell Sci.* 2004; 117(pt 24):5875–5886.
5. McGarry TJ, Kirschner MW. Geminin, an inhibitor of DNA replication, is degraded during mitosis. *Cell.* 1998;93:1043–1053.
6. Hodgson B, Li A, Tada S, Blow JJ. Geminin becomes activated as an inhibitor of Cdt1/RLF-B following nuclear import. *Curr Biol.* 2002;12:678–683.
7. Yoshida K, Takisawa H, Kubota Y. Intrinsic nuclear import activity of geminin is essential to prevent re-initiation of DNA replication in Xenopus eggs. *Genes Cells.* 2005;10:63–73.
8. Quinn LM, Herr A, McGarry TJ, Richardson H. The Drosophila geminin homolog: roles for geminin in limiting DNA replication, in anaphase and in neurogenesis. *Genes Dev.* 2001;15:2741–2754.
9. Ballabeni A, Melixetian M, Zamponi R, Masiero L, Marinoni F, Helin K. Human geminin promotes pre-RC formation and DNA replication by stabilizing CDT1 in mitosis. *EMBO J.* 2004;23:3122–3132.
10. Kulartz M, Kreitz S, Hiller E, Damoc EC, Przybylski M, Knippers R. Expression and phosphorylation of the replication regulator protein geminin. *Biochem Biophys Res Commun.* 2003;305:412–420.
11. Bravou V, Nishitani H, Song SY, Taraviras S, Varakis J. Expression of the licensing factors, Cdt1 and geminin, in human colon cancer. *Int J Oncol.* 2005;27:1511–1518.
12. Wharton SB, Hibberd S, Eward KL, et al. DNA replication licensing and cell cycle kinetics of oligodendroglial tumors. *Br J Cancer.* 200419;91:262–269.
13. Montanari M, Boninsegna A, Faraglia B, et al. Increased expression of geminin stimulates the growth of mammary epithelial cells and is a frequent event in human tumors. *J Cell Physiol.* 2005;202:215–222.
14. Wohlschlegel JA, Kutok JL, Weng AP, Dutta A. Expression of geminin as a marker of cell proliferation in normal tissues and malignancies. *Am J Pathol.* 2002;161:267–273.
15. Xouri G, Lygerou Z, Nishitani H, Pachnis V, Nurse P, Taraviras S. Cdt1 and geminin are down-regulated upon cell cycle exit and are over-expressed in cancer-derived cell lines. *Eur J Biochem.* 2004;271:3368–3378.
16. Shetty A, Loddo M, Fanshawe T, et al. DNA replication licensing and cell cycle kinetics of normal and neoplastic breast. *Br J Cancer.* 200528;93:1295–1300.

17. Gonzalez MA, Tachibana KE, Chin SF, et al. Geminin predicts adverse clinical outcome in breast cancer by reflecting cell-cycle progression. *J Pathol.* 2004;204:121–130.
18. Dudderidge TJ, Stoeber K, Loddo M, et al. Mcm2, geminin, and Ki67 define proliferative state and are prognostic markers in renal cell carcinoma. *Clin Cancer Res.* 2005;11: 2510–2517.
19. Ashby LS, Ryken TC. Management of malignant glioma: steady progress with multimodal approaches. *Neurosurg Focus.* 2006;20:E3.
20. Rainov NG, Soling A, Heidecke V. Novel therapies for malignant gliomas: a local affair? *Neurosurg Focus.* 2006; 20:E9.
21. Hama S, Matsuura S, Tauchi H, et al. p16 Gene transfer increases cell killing with abnormal nucleation after ionising radiation in glioma cells. *Br J Cancer.* 2003;89:1802–1811.
22. Terasima T, Tolmach LJ. Variations in several responses of HeLa cells to x-irradiation during the division cycle. *Biophys J.* 1963;3:11–33.

Reprinted from JOURNAL OF NEUROLOGY, NEUROSURGERY AND PSYCHIATRY, July 2007, Vol 78, p 716-721

PAPER

Clinical significance of preoperative fibre-tracking to preserve the affected pyramidal tracts during resection of brain tumours in patients with preoperative motor weakness

Nobuhiro Mikuni, Tsutomu Okada, Rei Enatsu, Yukio Miki, Shin-ichi Urayama, Jun A Takahashi, Kazuhiko Nozaki, Hidenao Fukuyama, Nobuo Hashimoto

J Neurol Neurosurg Psychiatry 2007;**78**:716–721. doi: 10.1136/jnnp.2006.099952

See end of article for authors' affiliations

Correspondence to: Dr Nobuhiro Mikuni, Department of Neurosurgery, Kyoto University Graduate School of Medicine, 54 Kawahara-cho, Shogoin, Sakyo-ku, Kyoto, 6068507, Japan; mikunin@kuhp.kyoto-u.ac.jp

Received 13 June 2006
Revised 6 October 2006
Accepted 7 February 2007
Published Online First 1 March 2007

Objective: To clarify the clinical usefulness of preoperative fibre-tracking in affected pyramidal tracts for intraoperative monitoring during the removal of brain tumours from patients with motor weakness.

Methods: We operated on 10 patients with mild to moderate motor weakness caused by brain tumours located near the pyramidal tracts under local anaesthesia. Before surgery, we performed fibre-tracking imaging of the pyramidal tracts and then transferred this information to the neuronavigation system. During removal of the tumour, motor function was evaluated with motor evoked potentials elicited by cortical/subcortical electrical stimulation and with voluntary movement.

Results: In eight patients, the locations of the pyramidal tracts were estimated preoperatively by fibre-tracking; motor evoked potentials were elicited on the motor cortex and subcortex close to the predicted pyramidal tracts. In the remaining two patients, in which fibre-tracking of the pyramidal tracts revealed their disruption surrounding the tumour, cortical/subcortical electrical stimulation did not elicit responses clinically sufficient to monitor motor function. In all cases, voluntary movement with mild to moderate motor weakness was extensively evaluated during surgery and was successfully preserved postoperatively with appropriate tumour resection.

Conclusions: Preoperative fibre-tracking could predict the clinical usefulness of intraoperative electrical stimulation of the motor cortex and subcortical fibres (ie, pyramidal tracts) to preserve affected motor function during removal of brain tumours. In patients for whom fibre-tracking failed preoperatively, awake surgery is more appropriate to evaluate and preserve moderately impaired muscle strength.

A number of anatomo-functional evaluations of the pyramidal tracts have been developed to help preserve motor function while maximising the removal of brain tumours located in close proximity to the pyramidal tracts. Integrated functional neuronavigation and preoperative neuroimaging, such as functional MRI (fMRI), magnetoencephalography (MEG) and fibre-tracking, have been combined with intraoperative electrical stimulation to establish the clinical significance of the findings of each evaluation method.[1–6] Despite these developments in mapping and monitoring techniques, little is known about their clinical utility for patients suffering from motor weakness caused by brain tumours. As the tolerance of affected pyramidal tracts for surgical manipulation is weaker in comparison with that in patients without motor weakness, intraoperative evaluation plays a critical role in the surgeon's ability to maintain motor function. Decreased motor function itself, however, may affect the accuracy of intraoperative evaluation.

White matter fibre-tracking using diffusion tensor imaging is capable of visualising the integrity of white matter.[1 4 7–11] Although fibre-tracking of the pyramidal tracts does not always correlate with the degree of motor weakness, it does reflect the functional condition of the fibres.[10] To predict the clinical usefulness of intraoperative evaluation by presurgical non-invasive fibre-tracking imaging in patients with motor weakness, we compared the results of pyramidal tract fibre-tracking with the results of intraoperative direct electrical stimulation of the motor cortex and subcortical fibres (ie, pyramidal tracts) and spontaneous movements.

PATIENTS AND METHODS

Patients

We examined 10 patients, aged 28–67 years, who suffered from mild to moderate preoperative motor weakness due to brain tumours located close to the pyramidal tracts (table 1). The tumours included five cases of glioblastoma multiforme, three of anaplastic astrocytoma, one of diffuse astrocytoma and one cavernoma. All lesions were located within the language dominant frontal lobe; before operation, five patients had mild motor aphasia. In response to stimulation of the bilateral median and tibial nerves, scalp somatosensory evoked potentials (SEPs) were recorded in all patients. To evaluate cortical activity during voluntary movement, we evaluated finger/foot tapping during fMRI and MEG studies.

MRI data acquisition and diffusion tensor imaging (DTI) data processing for fibre-tracking and fibre-tractography reconstruction

Detailed methods for fibre-tracking have been described elsewhere.[6 11] Preoperative DTI and anatomical T1/T2 weighted volume imaging used a 3 T MR scanner (Trio; Siemens, Erlangen, Germany). T1 weighted volume data were obtained using a three dimensional magnetisation prepared rapid gradient echo (MPRAGE) sequence. T2 weighted volume data

Abbreviations: DTI, diffusion tensor imaging; fMRI, functional MRI; MEG, magnetoencephalography; MEP, motor evoked potential; MPRAGE, magnetisation prepared rapid gradient echo; ROI, region of interest; SEP, somatosensory evoked potential

Table 1 Clinical characteristics of the 10 patients

Patient No	Age (y)	Sex	Histological type	Location
1	67	M	Glioblastoma multiforme	Left fronto-parietal
2	58	F	Glioblastoma multiforme	Left fronto-insulo-temporo-parietal
3	53	M	Anaplastic astrocytoma	Left fronto-parietal
4	28	M	Glioblastoma multiforme	Left fronto-parietal
5	40	F	Glioblastoma multiforme	Left frontal
6	40	F	Cavernoma	Left fronto-parietal
7	48	M	Diffuse astrocytoma	Left fronto-parietal
8	56	M	Anaplastic astrocytoma	Left frontal
9	60	F	Anaplastic astrocytoma	Left fronto-insulo-temporal
10	50	M	Glioblastoma multiforme	Right fronto-parietal

were obtained using a three dimensional true fast imaging with steady precession sequence. DtiStudio software was used to perform fibre-tractography based on the fibre-assignment by continuous tracking method.[9 14] Fibre-tracking was initiated in both retrograde and orthograde directions according to the direction of the principal eigenvector in each voxel. Results that penetrated the manually segmented regions of interest (ROIs) were assigned to specific tracts. To reconstruct the pyramidal tract, two ROIs were segmented on axial $b = 0$ images: the first ROI at the cerebral peduncles and the second ROI at the precentral gyri.[9 15 16] If the pyramidal tracts were not detected between the two ROIs because of the presence of tumours, the hyperintensity area at the internal capsule on the $b = 0$ image was selected as the second ROI.[11]

Fibre-tractography data processing for navigation system

To convert tractography into a DICOM format dataset, three processing steps were applied. The first step was to change tractography to a voxel dataset. An 8 bit voxel dataset with binary contrast was created from the original tractography using DtiStudio, with the same matrix size as $b = 0$ images. In this voxelised tractography, marked voxels where fibre-tracts penetrate displayed the largest value, and other voxels the smallest ones.[15] The second step was to create merged images of tractography and $b = 0$ images with the same matrix size as the MPRAGE images. The 3-orthogonal coordinates of each voxel in MPRAGE and $b = 0$ images were obtained from the DICOM header information. Trilinear interpolation was applied for voxel value calculation. Merged images were generated from interpolated tractography and interpolated $b = 0$ images. The third step was to convert merged images into DICOM format, according to the MPRAGE header information. DICOM format tractography with the same imaging matrices as MPRAGE were obtained.

Preparation in the navigation system

The MPRAGE images, fast imaging with steady precession images and DICOM format tractography images were transferred to the navigation system (StealthStation TRIA plus, Medtronic Sofamor-Danek, Memphis, Tennessee, USA; or Vector Vision Compact Navigation System, Brain LAB AG Heimstetten, Germany) using Cranial 4.0/VV Cranial 7.5 software. We then applied non-rigid image fusion based on a mutual information algorithm using ImMerge/iPlan2.5 software. The day before the operation, we performed axial whole brain CT with a contiguous slice thickness of 1 mm and six independent scalp point markers for anatomical registration. The CT dataset was also input into the navigation system. CT, MPRAGE and DICOM format tractography were automatically registered; the anatomical registration points were verified to minimise navigation errors. As the differences in distortion between DTI and MPRAGE were within a few millimetres according to a phantom for the neuronavigation system, we determined that the spatial accuracy of the single shot echo planar sequence would be reliable; the potential error of the navigation due to image distortions would be limited to a few millimetres. At navigation setup, the accuracy of image registration was less than 2 mm. Fibre-tracking tractography

Table 2 Results of evaluation of motor function by preoperative and intraoperative assessments

Patient No	Motor weakness	MEG	fMRI	Scalp SEP	Fibre-tracking	MEPs (cortex)	MEPs (subcortex)	Awake surgery
1	Hand 4/5	x	x	x	x	o (unstable)	x	o
	Bracjium 3/5	x	x	x	x	x	x	o
	Leg 2/5	x	x	x	x	x	x	o
2	Hand, bracjium 1/5	x	x	x	x	x	x	o
	Leg 4/5	x	x	x	x	x	o (<1 cm)	o
3	Hand, bracjium 3/5	o	o	o	o	o	o (<1 cm)	o
4	Hand 4/5	o	o	o	o	o	o (<1 cm)	o
5	Hand 4/5	NA	NA	o	o	o	o (<1 cm)	o
6	Hand 4/5	o	o	o	o	o	o (<1 cm)	o
7	Hand, bracjium 4/5	NA	o	o	o	o	o (<1)	o
8	Hand 4/5	NA	NA	o	o	o	x (>2 cm)	o
9	Hand 4/5	o	NA	o	o	o	x (1 cm<<2 cm)	o
10	Hand 4/5	NA	o	o	o	o	x (1 cm<<2 cm)	o

fMRI, functional magnetic resonance imaging; MEG, magnetoencephalography; MEP, motor evoked potential; NA, not available; o, motor function detected; SEP, somatosensory evoked potentials; x, motor function was undetected.
The distances between points of subcortical stimulation and the fibre-tracking pyramidal tracts are shown as less than 1 cm (<1 cm), between 1 and 2 cm (1 cm<<2 cm) or more than 2 cm (>2 cm).

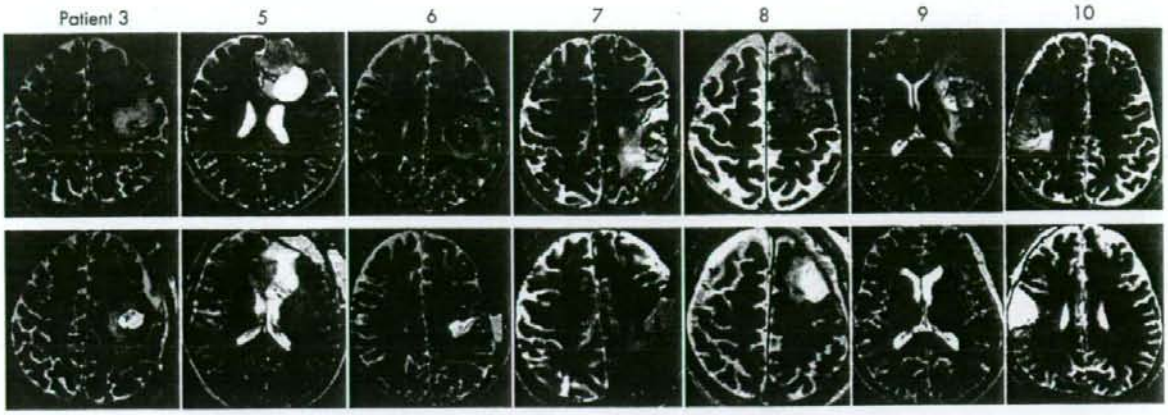

Figure 1 Upper: preoperative T2 weighted MRI in patient Nos 3, 5, 6, 7, 8, 9 and 10, with brain tumours showing a hyperintense area that is close to the pyramidal tracts (red), identified by fibre-tracking. Lower: postoperative T2 weighted MRI demonstrated the extent of tumour removal. Postoperative fibre-tracking in patient Nos 3, 6 and 9 revealed preservation of the pyramidal tracts (red).

of the pyramidal tracts between the cerebral peduncle and the precentral gyrus was successful in 50 surgically treated brain tumour patients without motor weakness (data not shown).

Intraoperative electrical stimulation

The bilateral abductor pollicis brevis, biceps brachialis, deltoid, gastrocnemius, quadriceps femoris and tibialis anterior muscles were chosen for electromyogram recording using neurological monitoring (Epoch XP, Axon Systems, New York, USA). After induction, general anaesthesia was maintained by intravenous infusion with propofol for craniotomy. Muscle relaxants were administered only for intubation and were not continued during surgery. The highest N20–P20 phase reversal of cortical SEPs was recorded using 4×5 subdural electrodes to identify the central sulcus. If SEPs were not sufficient to define the central sulcus, intraoperative visual inspection of the sulci combined with neuronavigation was used to orient the anatomy. After discontinuing the propofol infusion, patients awoke without further deficits.

To monitor motor function of the corticospinal tracts electrophysiologically, we first stimulated the precentral gyrus to identify a positive control motor evoked potential (MEP) and the intensity appropriate to stimulate subcortical fibres. The intensity of cortical stimulation was increased from 5 mA to a maximum of 25 mA. If afterdischarges were induced, we repeated the test at the same intensity or using a 1 mA lower

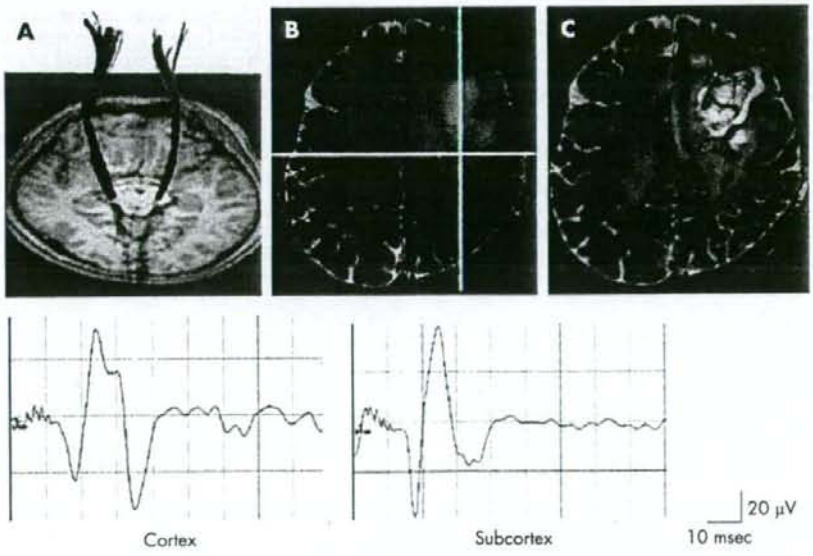

Figure 2 Patient No 4 had a left fronto-parietal glioblastoma multiforme. (A) Preoperative fibre-tracking identified symmetrical pyramidal tracts (red lines) from the cortex to the cerebral peduncles. (B) Brain T2 weighted MRI revealed a hyperintense area in close proximity to the left pyramidal tract, identified by fibre-tracking (red). Cortical stimulation of the left precentral gyrus, which had been defined by a somatosensory evoked potential, elicited a motor evoked potential (MEP) in the right abductor pollicis brevis muscle (Cortex). During removal of the tumour, subcortical stimulation elicited MEPs at the bottom of the tumour (intersection of the yellow lines in the intraoperative navigation image), 1 cm from the edge of the predicted pyramidal tract (red) (Subcortex). To avoid causing additional neurological deficits, no further removal was performed. (C) Postoperative T2 weighted MRI demonstrated preservation of the pyramidal tracts identified by fibre-tracking (red).

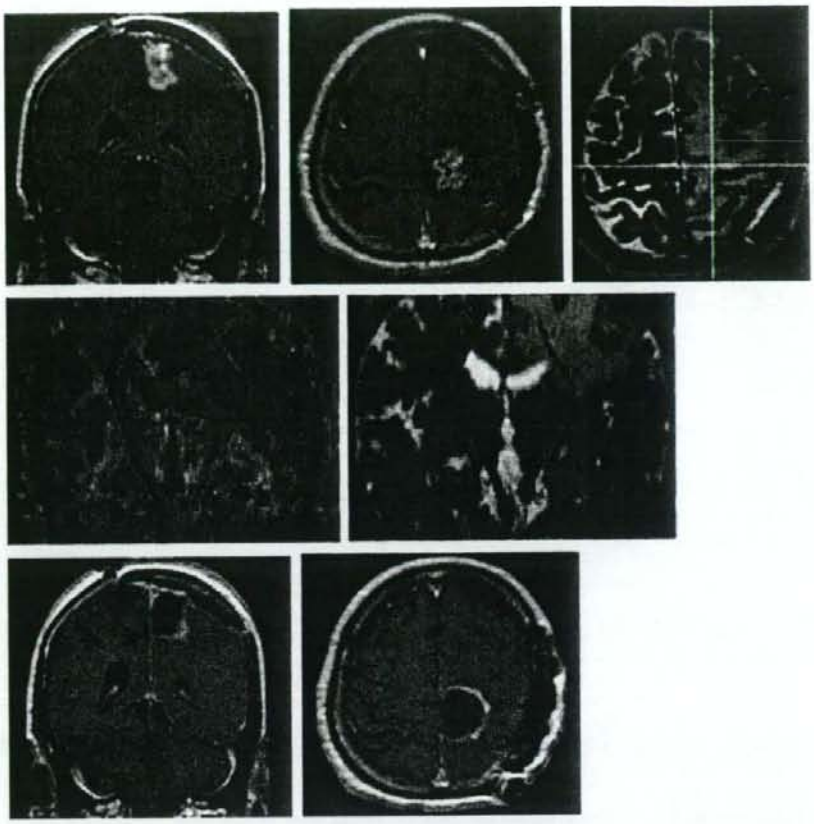

Figure 3 Patient No 1. Fibre-tracking of the pyramidal tracts was disrupted in a 67-year-old man with a left fronto-parietal glioblastoma multiforme. Upper: preoperative T2 weighted MRI identified a focus of hyperintensity in the left perirolandic region with gadolinium enhancement of the rostral precentral cortex. Stimulation of the left cortex rarely elicited weak motor evoked potential (MEP) responses on the right abductor pollicis brevis muscle. Subcortical stimuli, even on the approximated posterior bank of the precentral gyrus on neuronavigation (intersection of the yellow lines in the intraoperative navigation image), did not elicit MEPs. Middle: a relative anisotropy map indicated the principal eigenvector (green, anterior–posterior; red, right–left; and blue, inferior–superior). Fibre-tracking of the left pyramidal tracts (red lines) near the tumour was disrupted during its course to the cortex. Lower: postoperative MRI with gadolinium enhancement.

current. During removal of tumour tissue within 2 cm of the pyramidal tracts by intraoperative neuronavigation, we performed repetitive subcortical electrical stimulations. Electrical stimuli were applied across a relatively wide area to avoid any anatomical shift caused by the tumour. Five trains of monophasic square waves with a duration of 0.2 ms were applied. Current was delivered by a pair of adjacent electrodes (3 mm in diameter) with a centre-to-centre inter-electrode distance of 1 cm.[3] A 50 Hz electric current was delivered for language and sensory testing. Language functions were assessed by the reading of a paragraph, spontaneous speech, naming and comprehension activities.[17] We confirmed the points of stimulation by visualisation using the navigation system. In all patients, the minimum distances between points of stimulation and the fibre-tracking pyramidal tracts were measured using three dimensional MRI by intraoperative neuronavigation.

Surgery

All patients underwent removal of their tumour under local anaesthesia using the combination of tractography integrated functional neuronavigation and direct cortical/subcortical stimulation. During removal of the tumours around the pyramidal tracts, motor function of all four extremities was continuously monitored using the muscle manoeuvre test.[18] Language function was evaluated using similar testing as that used for electrical stimulation, depending on the location of the tumour. In three patients in whom part of the tumour extended into the left angular gyrus, single digit multiplication was evaluated. All procedures were approved by the ethics committee (No 542); written informed consent was obtained from all patients. As the presence of subcortical MEPs during resection of the tumour is an important sign warning of permanent motor weakness, we avoided further resection after obtaining the first MEP response.[19 20]

RESULTS

Results of evaluation of motor function by preoperative and intraoperative assessments are summarised in table 2. Preoperative fibre-tracking identified the pyramidal tracts of eight patients, including seven with mild hand motor weakness (patient Nos 4–10) and one with moderate motor weakness (3/5) of his upper limb (patient No 3) (figs 1, 2). In all patients, MEPs were elicited for all of the muscles evaluated, including the weakened muscles, by electrical stimulation of both the precentral gyrus and the subcortex within 1 cm of the pyramidal tracts, identified by intraoperative functional neuronavigation. The tumours were removed while confirming stable MEP responses by repetitive electrical stimulation. Motor function was either

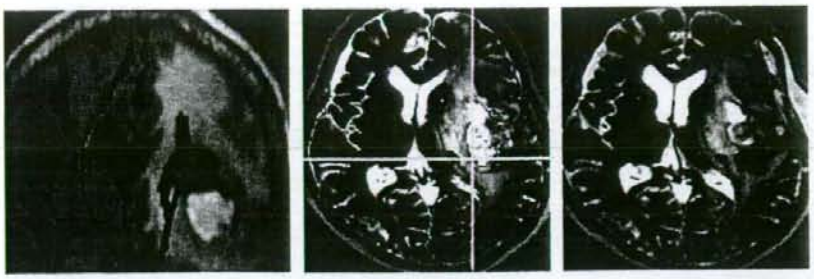

Figure 4 Patient No 2. Left: fibre-tracking of the pyramidal tracts (red lines) demonstrated disruption around a left fronto-insulo-temporo-parietal glioblastoma multiforme. Middle: during removal of the tumour, cortical stimuli did not elicit any motor evoked potentials (MEPs). Subcortical stimuli very close to the predicted pyramidal tracts (red) on neuronavigation (intersection of the yellow lines in an intraoperative navigation image), however, elicited MEPs of her affected right lower extremities, but not her right upper extremities. Right: Postoperative T2 weighted MRI demonstrated that the pyramidal tracts identified by fibre-tracking (red) were preserved.

maintained or improved both during and after the operation. In addition, we demonstrated preservation of the pyramidal tracts by postoperative fibre-tracking (patient Nos 3, 4, 6 and 9).

In two patients (patient Nos 1 and 2), fibre-tracking of the pyramidal tracts around the tumour failed. Patient No 1 (fig 3) suffered from preoperative right hemiparesis (3/5 on the brachium, 4/5 on the hand and 2/5 on the leg) because of left fronto-parietal glioblastoma multiforme. Cortical SEPs exhibited weak responses on stimulation of the right median nerve; no response was observed after stimulation of the right tibial and sural nerves. Cortical stimulation of the anatomically confirmed precentral gyrus by neuronavigation elicited a rare MEP in his abductor pollicis brevis muscle; no MEPs were elicited in his biceps brachialis, deltoid, gastrocnemius, quadriceps femoris or tibialis anterior muscles. Neurological examinations soon after the patient recovered from general anaesthesia demonstrated no additional deficits. As the tumour was removed piece by piece, continuous evaluation of muscle strength helped preserve motor function of the lower extremities and improve motor function of the upper extremities to 4/5. Subcortical electrical stimulation did not elicit MEPs at any point during resection of the tumour. Patient No 2 (fig 4) exhibited right hemiparesis (1/5 on the upper extremity and 4/5 on the leg) preoperatively, caused by a left fronto-insulo-temporo-parietal glioblastoma multiforme. We operated on this patient with the goal of preserving motor function of the lower extremities. She also displayed mild motor aphasia. Cortical SEPs could not be elicited. Despite the absence of MEP responses following cortical stimulation of the wide area surrounding the anatomically identified precentral gyrus by neuronavigation, subcortical stimulation elicited MEPs of her lower but not upper extremities. Through continuous evaluation of muscle strength intraoperatively, motor function of the lower extremities was preserved during removal of the tumour. Postoperatively, she exhibited adequate removal of the tumour without any further neurological deficits.

DISCUSSION

To maintain the quality of life of patients with motor weakness undergoing surgical treatment of brain tumours, it is essential to evaluate motor function intraoperatively. The damage done to the pyramidal tracts, however, may affect the results of the evaluation. As MEPs elicited by direct intraoperative electrical stimulation remain the most reliable index of motor function,[21–23] it is important to predict if MEP responses will be elicited from the affected motor cortex and the pyramidal tracts during removal of the tumour. Presurgical evaluations, such as the degree of motor weakness (muscle strength), MEG, fMRI, positron emission tomography, transcranial magnetic stimulation and fibre-tracking are all potential candidates for predicting intraoperative MEP responses.

In this study, the degree of preoperative motor weakness did not always correlate with the incidence of intraoperative MEP responses. Muscles that were moderately affected by compression caused by the tumour elicited MEPs following cortical/subcortical stimulation (patient No 3), a result that is consistent with previous case reports.[2 24] MEP responses, however, could not be elicited from only mildly affected muscles in two patients (patient Nos 1 and 2). MEG, fMRI and positron emission tomography images provide information concerning motor function at the cortical, but not subcortical, level. Repetitive voluntary movements are often necessary to elicit motor evoked fields by MEG and bold effects by fMRI. While preoperative scalp SEPs correlated with the incidence of MEP responses in our patients, the results of SEP assessments do not directly reflect motor function.

Fibre-tracking of the affected pyramidal tracts was first compared with the incidence of intraoperative MEP responses by direct cortical/subcortical electrical stimulation. Subcortical MEPs were always elicited in regions in close proximity to the pyramidal tracts that had been predicted by fibre-tracking in patients with mild to moderate preoperative motor weakness. In addition, continuous fibre-tracking of the pyramidal tracts from the motor cortex to the cerebral peduncle indicated the positive response of cortical MEPs. On the other hand, cortical MEPs were never elicited as reliable responses in patients with disrupted fibre-tracking pyramidal tracts. These data suggest that preoperative fibre-tracking of the pyramidal tracts provides anatomical information as well as functional information in predicting the clinical usefulness of intraoperative cortical/subcortical electrical stimulation.

Several limitations to fibre-tracking as a preoperative evaluation, however, should be mentioned. Selection of the seed ROIs and the thresholding of fractional anisotropy, which define the parameter of the algorithm used in the procedure, may subjectively affect the errors in track trajectories.[8 25 26] In the present study, individual muscle maintained various degrees of motor activity preoperatively instead of disruption on the fibre-tracking pyramidal tracts, which may reflect the limitations of fibre-tracking from technical errors and pathological conditions. Part of the pyramidal fibres tracking from the precentral gyrus in lower convexity may fail to trace the precise course because the pyramidal tract intersects with callosal fibres and the superior longitudinal fasciculus at the level of the centrum semiovale.[3 27 28] Lack of visualisation of some upper limb fibres would account for some of the discrepancies between extent of weakness and ability to visualise fibres. To compare the pyramidal fibres tracking and MEP responses more precisely, taking intraoperative brain shift[29]

into consideration. DTI image processing during the course of surgery with the use of intraoperative MRI is needed.[5 30 31] In addition, individual pathophysiological factors resulting from the brain tumours may affect the results of fibre-tracking,[2 10 20 32 33] although it is controversial whether the tumour itself or peritumoral oedema on the pyramidal tracts can be distinguished by DTI metrics.[34 35] In the two such patients evaluated in this study, preservation of motor function indicated that secondary effects, such as oedema or mass effect, rather than tumour infiltration, caused the motor deficits. Relatively large amounts of peritumoral oedema in these patients compared with the other eight patients might cause unsuccessful fibre-tracking of the pyramidal tracts. Although a wide area was stimulated electrically, a portion of the pyramidal tracts may have been shifted by compression of the tumour. Further studies with a larger number of patients will be necessary to study the physiological significance of fibre-tracking of affected pyramidal tracts and to clarify the clinical relationship between preoperative fibre-tracking and intraoperative cortical/subcortical electrical stimulation. The tendency for patients not to be operated on until they begin to suffer from moderate motor weakness due to growing brain tumours may, however, limit these studies. In addition, post-operative fibre-tracking of the pyramidal tracts and neurological status should be compared with the extent of tumour resection for further verification of the clinical value of preoperative fibre-tracking.

Despite the clinical utility of complete pyramidal tract fibre-tracking in reliable MEPs of the motor cortex and pyramidal tracts, disruption of estimated pyramidal tracts suggested that electrical stimulation is insufficient to permit the preservation of motor function during tumour removal. For patients with mild to moderate motor weakness in whom pyramidal tract fibre-tracking failed preoperatively, awake surgery would be better suited to evaluate motor function by voluntary movement during removal of the tumour. As awake surgery allows spontaneous movements to be easily monitored continuously, it would be useful for a subset of pathological conditions.[36] During removal of a tumour under local anaesthesia, injuries to motor associated areas must also be considered. Motor weakness is not observed immediately after resection of the supplementary motor area[37] whereas an injury to the negative motor area after resection would cause an immediate and transient disturbance in fine movement.[17]

Authors' affiliations

Nobuhiro Mikuni, Rei Enatsu, Jun A Takahashi, Kazuhiko Nozaki, Nobuo Hashimoto, Department of Neurosurgery, Kyoto University Graduate School of Medicine, Kyoto, Japan

Tsutomu Okada, Yukio Miki, Department of Diagnostic Imaging and Nuclear Medicine, Kyoto University Graduate School of Medicine, Kyoto, Japan

Shin-ichi Urayama, Hidenao Fukuyama, Human Brain Research Centre, Kyoto University Graduate School of Medicine, Kyoto, Japan

Competing interests: None.

REFERENCES

1 **Coenen VA**, Krings T, Axer H, *et al.* Intraoperative three-dimensional visualization of the pyramidal tract in a neuronavigation system (PTV) reliably predicts true position of principal motor pathways. *Surg Neurol* 2003;**60**:381–90.
2 **Kamada K**, Todo T, Masutani Y, *et al.* Combined use of tractography-integrated functional neuronavigation and direct fiber stimulation. *J Neurosurg* 2005;**102**:664–72.
3 **Mikuni N**, Oakado T, Nishida N, *et al.* Comparison between motor evoked potential and fiber tracking for estimating pyramidal tracts near brain tumors. *J Neurosurg* 2007;**106**:128–33.
4 **Nimsky C**, Ganslandt O, Fahlbusch R. Implementation of fiber tract navigation. *Neurosurgery* 2006;**58**:292–304.
5 **Nimsky C**, Ganslandt O, Buchfelder M, *et al.* Intraoperative visualization for resection of gliomas: the role of functional neuronavigation and intraoperative 1.5 T MRI. *Neurol Res* 2006;**28**:482–7.
6 **Okada T**, Mikuni N, Miki et al. Corticospinal tract localization: integration of diffusion-tensor tractography at 3-T MR imaging with intraoperative white matter stimulation mapping—preliminary results. *Radiology* 2006;**240**:849–57.
7 **Hendler T**, Pianka P, Sigal M, *et al.* Delineating gray and white matter involvement in brain lesions: three-dimensional alignment of functional magnetic resonance and diffusion-tensor imaging. *J Neurosurg* 2003;**99**:1018–27.
8 **Mori S**, Crain BJ, Chacko VP, *et al.* Three-dimensional tracking of axonal projections in the brain by magnetic resonance imaging. *Ann Neurol* 1999;**45**:265–9.
9 **Wakana S**, Jiang H, Nagae-Poetscher LM, *et al.* Fiber tract-based atlas of human white matter anatomy. *Radiology* 2004;**230**:77–87.
10 **Witwer BP**, Moftakhar R, Hasan KM, *et al.* Diffusion-tensor imaging of white matter tracts in patients with cerebral neoplasm. *J Neurosurg* 2002;**97**:568–75.
11 **Yagishita A**, Nakano I, Oda M, *et al.* Location of the corticospinal tract in the internal capsule at MR imaging. *Radiology* 1994;**191**:455–60.
12 **Lee JS**, Han MK, Kim SH, *et al.* Fiber tracking by diffusion tensor imaging in corticospinal tract stroke: Topographical correlation with clinical symptoms. *Neuroimage* 2005;**26**:771–6.
13 **Okada T**, Miki Y, Fushimi Y, *et al.* Diffusion-tensor fiber tractography: intraindividual comparison of 3.0-T and 1.5-T MR imaging. *Radiology* 2006;**238**:668–78.
14 **Jiang H**, van Zijl PC, Kim J, *et al.* DtiStudio: resource program for diffusion tensor computation and fiber bundle tracking. *Comput Methods Programs Biomed* 2006;**81**:106–16.
15 **Nagonawa S**, Koshikawa T, Kawai H, *et al.* Optimization of diffusion-tensor MR imaging data acquisition parameters for brain fiber tracking using parallel imaging at 3 T. *Eur Radiol* 2004;**14**:234–8.
16 **Yamada K**, Kizu O, Mori S, *et al.* Brain fiber tracking with clinically feasible diffusion-tensor MR imaging: initial experience. *Radiology* 2003;**227**:295–301.
17 **Mikuni N**, Ohara S, Ikeda A, *et al.* Evidence for a wide distribution of negative motor areas in the perirolandic cortex. *Clin Neurophysiol* 2006;**117**:33–40.
18 **Dejong RN**. Case taking and the neurological examination. In: Barker AB, eds. *Clinical neurology*. New York: Hoeber-Harper, 1955:1–100.
19 **Keles GE**, Lundin DA, Lamborn KR, *et al.* Intraoperative subcortical stimulation mapping for hemispherical perirolandic gliomas located within or adjacent to the descending motor pathways: evaluation of morbidity and assessment of functional outcome in 294 patients. *J Neurosurg* 2004;**100**:369–75.
20 **Kinoshita M**, Yamada K, Hashimoto N, *et al.* Fiber-tracking does not accurately estimate size of fiber bundle in pathological condition: initial neurosurgical experience using neuronavigation and subcortical white matter stimulation. *Neuroimage* 2005;**25**:424–9.
21 **Duffau H**. Lessons from brain mapping in surgery for low-grade glioma: insights into associations between tumour and brain plasticity. *Lancet Neurol* 2005;**4**:476–86.
22 **Kombos T**, Suess O, Ciklatekerlio O, *et al.* Monitoring of intraoperative motor evoked potentials to increase the safety of surgery in and around the motor cortex. *J Neurosurg* 2001;**95**:608–14.
23 **Neuloh G**, Pechstein U, Cedzich C, *et al.* Motor evoked potential monitoring with supratentorial surgery. *Neurosurgery* 2004;**54**:1061–72.
24 **Duffau H**. Recovery from complete hemiplegia following resection of a retrocentral metastasis: the prognostic value of intraoperative cortical stimulation. *J Neurosurg* 2001;**95**:1050–2.
25 **Clark CA**, Barrick TR, Murphy MM, *et al.* White matter fiber tracking in patients with space-occupying lesions of the brain: a new technique for neurosurgical planning? *Neuroimage* 2003;**20**:1601–8.
26 **Lin CP**, Tseng WY, Cheng HC, *et al.* Validation of diffusion tensor magnetic resonance axonal fiber imaging with registered manganese-enhanced optic tracts. *Neuroimage* 2001;**14**:1035–47.
27 **Berman JI**, Berger MS, Mukherjee P, *et al.* Diffusion-tensor imaging-guided tracking of fibers of the pyramidal tract combined with intraoperative cortical stimulation mapping in patients with gliomas. *J Neurosurg* 2004;**101**:66–72.
28 **Wiegell MR**, Larsson HB, Wedeen VJ. Fiber crossing in human brain depicted with diffusion tensor MR imaging. *Radiology* 2000;**217**:897–903.
29 **Reinges MH**, Nguyen HH, Krings T, *et al.* Course of brain shift during microsurgical resection of supratentorial cerebral lesions: limits of conventional neuronavigation. *Acta Neurochir (Wien)* 2004;**146**:369–77.
30 **Nimsky C**, Ganslandt O, Hastreiter P, *et al.* Intraoperative diffusion-tensor MR imaging: shifting of white matter tracts during neurosurgical procedures—initial experience. *Radiology* 2005;**234**:218–25.
31 **Nimsky C**, Ganslandt O, Hastreiter P, *et al.* Preoperative and intraoperative diffusion tensor imaging-based fiber tracking in glioma surgery. *Neurosurgery* 2005;**56**:130–8.
32 **Beppu T**, Inoue T, Kuzu Y, *et al.* Utility of three-dimensional anisotropy contrast magnetic resonance axonography for determining condition of the pyramidal tract in glioblastoma patients with hemiparesis. *J Neurooncol* 2005;**73**:137–44.
33 **Laundre BJ**, Jellison BJ, Badie B, *et al.* Diffusion tensor imaging of the corticospinal tract before and after mass resection as correlated with clinical motor findings: preliminary data. *AJNR Am J Neuroradiol* 2005;**26**:791–6.
34 **Lu S**, Ahn D, Johnson G, *et al.* Diffusion-tensor MR imaging of intracranial neoplasia and associated peritumoral edema: introduction of the tumor infiltration index. *Radiology* 2004;**232**:221–8.
35 **Provenzale JM**, McGraw P, Mhatre P, *et al.* Peritumoral brain regions in gliomas and meningiomas: investigation with isotropic diffusion-weighted MR imaging and diffusion-tensor MR imaging. *Radiology* 2000;**232**:451–60.
36 **Mikuni N**, Ikeda A, Yoneko H, *et al.* Surgical resection of an epileptogenic cortical dysplasia in the deep foot sensorimotor area: a case report. *Epilepsy Behav* 2005;**7**:559–62.
37 **Duffau H**, Lopes M, Denvil D, *et al.* Delayed onset of the supplementary motor area syndrome after surgical resection of the mesial frontal lobe: a time course study using intraoperative mapping in an awake patient. *Stereotact Funct Neurosurg* 2001;**76**:74–82.

J Neurosurg 106:593–598, 2007

Clinical impact of integrated functional neuronavigation and subcortical electrical stimulation to preserve motor function during resection of brain tumors

NOBUHIRO MIKUNI, M.D., PH.D.,[1] TSUTOMU OKADA, M.D.,[2] REI ENATSU, M.D.,[1] YUKIO MIKI, M.D., PH.D.,[2] TAKASHI HANAKAWA, M.D., PH.D.,[3] SHIN-ICHI URAYAMA, PH.D.,[3] KENICHIRO KIKUTA, M.D., PH.D.,[1] JUN A. TAKAHASHI, M.D., PH.D.,[1] KAZUHIKO NOZAKI, M.D., PH.D.,[1] HIDENAO FUKUYAMA, M.D., PH.D.,[3] AND NOBUO HASHIMOTO, M.D., PH.D.[1]

[1]Department of Neurosurgery, [2]Diagnostic Imaging and Nuclear Medicine, and [3]Human Brain Research Center, Kyoto University Graduate School of Medicine, Kyoto, Japan

Object. The authors evaluated the clinical impact of combining functional neuronavigation with subcortical electrical stimulation to preserve motor function following the removal of brain tumors.

Methods. Forty patients underwent surgery for treatment of brain tumors located near pyramidal tracts that had been identified by fiber tracking. The distances between the electrically stimulated white matter and the pyramidal tracts were measured intraoperatively with tractography-integrated functional neuronavigation, and correlated with subcortical motor evoked potentials (MEPs) and clinical symptoms during and after resection of the tumors.

Motor function was preserved after appropriate tumor resection in all cases. In 18 of 20 patients, MEPs were elicited from the subcortex within 1 cm of the pyramidal tracts as measured using intraoperative neuronavigation. During resection, improvement of motor weakness was observed in two patients, whereas transient mild motor weakness occurred in two other patients. In 20 patients, the distances between the stimulated subcortex and the estimated pyramidal tracts were more than 1 cm, and MEPs were detected in only three of these patients following stimulation.

Conclusions. Intraoperative functional neuronavigation and subcortical electrical stimulation are complementary techniques that may facilitate the preservation of pyramidal tracts around 1 cm of resected tumors.

KEY WORDS • pyramidal tract • fiber tracking • motor evoked potential • motor function • neuronavigation

PRESERVING motor function while maximizing brain tumor resection is a major goal of neurosurgery. Presurgical noninvasive functional imaging, including positron emission tomography, functional MR imaging, and magnetoencephalography, enables the visualization of cortical areas involved in motor function, and has been integrated into functional neuronavigation. Cortical and subcortical functional connectivity can be clarified using intraoperative electrical stimulation.[9] To define the subcortical fibers from the primary motor cortex (the pyramidal tracts) as well as to monitor their motor function, MEPs elicited by direct electrical stimulation remain the most reliable index. Despite the use of presurgical cortical functional mapping and evaluation of MEPs, 7 to 20% of patients with perirolandic tumors suffer permanent motor weakness postoperatively, mainly due to resection of subcortical lesions near the pyramidal tracts.[3,8,15]

The fiber-tracking technique based on DT imaging shows the 3D macroscopic architecture of fiber tracts.[6,12,21,30,31] Recently, investigators have developed a new method for anatomofunctional mapping, using tractography-integrated functional neuronavigation combined with direct fiber electrical stimulation (MEP recording).[5,14,24] We have reported on the use of this method by using 3-tesla MR imaging.[26] To understand the clinical impact of this new technique on motor outcome during the resection of brain tumors located near the pyramidal tracts, we have directly compared the results of fiber tracking and subcortical electrical stimulation during intraoperative neuronavigation. Neurological evaluations of motor function were performed during the surgery and postoperatively.

Clinical Material and Methods

All procedures were approved by the ethics committee, and written informed consent was obtained from all patients.

Patient History

We examined 40 patients, 15 to 69 years of age, with

Abbreviations used in this paper: CT = computed tomography; DICOM = digital imaging and communications in medicine; DT = diffusion-tensor; MEP = motor evoked potential; MPRAGE = magnetization prepared rapid gradient echo; MR = magnetic resonance; ROI = region of interest.

tumors located close to the pyramidal tracts. These tumors included one pilocytic astrocytoma, 10 diffuse astrocytomas, 14 anaplastic astrocytomas, eight glioblastomas multiforme, two oligodendrogliomas, one ependymoma, and four cavernomas (Table 1). In all patients, the lesion margins were less than 2 cm from the pyramidal tracts identified by preoperative fiber tracking. Mild motor weakness was observed preoperatively in five patients.

TABLE 1

Summary of the clinical characteristics of 40 patients with brain tumors

Tumor Type & Location	No. of Patients
histological type	
pilocytic astrocytoma	1
diffuse astrocytoma	10
anaplastic astrocytoma	14
glioblastoma multiforme	8
oligodendroglioma	2
ependymoma	1
cavernoma	4
anatomical location (rt/lt)	
frontal lobe	4/16
temporal lobe	2/5
insular cortex	2/5
parietal lobe	2/2
brainstem	2

Diffusion-Tensor Data Acquisition and Processing for Fiber Tracking

Detailed methods used in fiber tracking have been described elsewhere by one of the authors.[25,26] A whole-body 3-tesla MR imager (Trio, Siemens) was used to perform preoperative DT imaging as well as anatomical T_1- and T_2-weighted volume imaging. The T_1-weighted volume data were obtained using a 3D MPRAGE sequence, and the T_2-weighted volume data were obtained using a 3D true fast imaging with steady-state precession sequence.

Fiber Tractography Data Processing for use in the Navigation System

Fiber tracking was performed using all pixels inside the brain (that is, with the brute force approach) and was begun in both the orthograde and retrograde directions, according to the direction of the principal eigenvector in each voxel. Results that penetrated the manually segmented ROIs based on the known anatomical distributions of tracts were assigned to those specific tracts. To reconstruct the pyramidal tract using tractography, two ROIs were segmented on axial non–diffusion weighted images: the first ROI at both cerebral peduncles, and the second ROI at both precentral gyri.[21,26,31]

In the process of converting tractography data into a DICOM-format data set, three steps were used. In the first step, tractography data were changed into a voxel data set. Using DtiStudio software version 2.02 (H. Jiang, S. Mori: Department of Radiology, Johns Hopkins University), an 8-bit voxel data set with binary contrast was created from the original tractography data with the same matrix size as non–diffusion weighted images. In this voxelized tractography data set, marked voxels (where fiber tracts showed penetration) showed the largest value, whereas other voxels displayed the smallest value.[19]

In the second step, tractographic images and non–diffusion weighted images were merged, using the same matrix size as that for MPRAGE images. The three orthogonal coordinates of each voxel on MPRAGE and non–diffusion weighted images were obtained from the DICOM header information. To calculate voxel values, trilinear interpolation was used. Merged images were generated from interpolated tractographic images and interpolated non–diffusion weighted images.

In the third step, merged images were converted into DICOM format according to the MPRAGE header information. Tractography studies in DICOM format with the same imaging matrices as MPRAGE studies were obtained.

Preparation in the Navigation System

The MPRAGE images, fast imaging with steady-state precession images, and DICOM-format tractography images were transferred to the navigation system (StealthStation TRIA plus with Cranial 4.0 software, Medtronic Sofamor-Danek; or Vector Vision Compact Navigation System with VV Cranial 7.5 software, BrainLab AG). We applied nonrigid image fusion to the images using ImMerge or iPlan 2.5 software, based on a mutual information algorithm. The day before the operation, we performed axial whole brain CT with a contiguous slice thickness of 1 mm by attaching six independent scalp point markers to the patient for anatomical registration. The CT image data set was also transferred to the navigation system. Computed tomography images, MPRAGE images, and DICOM-format tractography were registered automatically, and the anatomical registration points were verified to minimize navigation error. The differences in distortions between DT imaging and MPRAGE imaging were within a few millimeters according to our study using a phantom for the neuronavigation system, and therefore spatial accuracy of the single-shot echo planar sequence would be reliable. The potential for error during neuronavigation due to image distortions would be limited to a few millimeters. The accuracy of image registration was within 2 mm at navigation setup.

Intraoperative Electrical Stimulation

The bilateral abductor pollicis brevis, biceps, brachialis, deltoid, gastrocnemius, quadriceps femoris, and tibialis anterior muscles were selected for electromyographic recording by using neurological monitoring (Epoch XP, Axon Systems). General anesthesia was induced and maintained with intravenous infusion of propofol during the craniotomy. Muscle relaxants were administered only for intubation procedures and not during surgery. A peripheral nerve stimulator was used to confirm train-of-four muscle contractions. To identify the central sulcus, the highest N20 to P20 phase reversal of somatosensory evoked potentials was recorded using 4 × 5 subdural electrodes. For electrophysiologically monitoring the motor function of corticospinal tracts, the precentral gyrus was first stimulated to identify a positive control MEP as well as the intensity that was to be further used to stimulate the subcortical fiber. The intensity for cortical stimulation was increased by 1-mA increments, from 5 mA to a maximum of 15 mA. If afterdischarges